January 2024

Research Project Report
Aluminum Life Cycle in Process of Hydrogen and Electric Energy Production from Aluminum-Water Reaction

Elinor Kostjukovsky

Advisor: Prof. Alon Gany

Faculty of Aerospace Engineering, Technion - Israel Institute of Technology

Abstract

This report provides an overview of the essential processes and factors involved in aluminum production, emphasizing the energy and life cycle cost. There are two types of aluminum, primary and secondary (or recycled). The production of primary aluminum involves two key processes: the Bayer process and the Hall-Héroult process. The Bayer process refines bauxite into aluminum oxide through stages such as crushing, digestion, clarification, precipitation, and calcination. The Hall-Héroult process involves electrolysis in specialized cells, featuring carbon anodes immersed in a bath solution. This process includes cell preparation, electrolysis, carbon dioxide release, and continuous operation.

Additionally, the report addresses the atomization process in aluminum production and its energy requirements. The project delves into a comprehensive review of mathematical and experimental models for gas atomization, focusing on non-ferrous metals, particularly aluminum.

Introduction

The request for sustainable and environmentally friendly energy sources has led to a growing interest in hydrogen as an alternative fuel. With its high reaction energy and benign byproducts, hydrogen presents a promising solution to the challenges posed by traditional fossil fuels. However, the widespread adoption of hydrogen as a fuel source has

been hindered by difficulties in its storage and transportation, primarily due to its low density and high reactivity. Addressing these challenges requires innovative approaches to hydrogen production that are efficient, cost-effective, and environmentally friendly. The objective of this report is to highlight and evaluate specific energy and cost aspects involved in the production of hydrogen from the reaction of aluminum and water:

$$Al + 3H_2O \rightarrow Al(OH)_3 + \frac{3}{2}H_2$$

Aluminum metal is naturally covered by a thin oxide layer, protecting it from further reaction with surrounding oxidizing atmosphere (air) or water. Rosenband and Gany [1] and Elitzur, Rosenband and Gany [2] proposed and investigated a patented process for activation of aluminum to react spontaneously with water for hydrogen production.
To ensure extensive reaction, the surface area of the activated aluminum must be sufficiently large. This is generally done by atomization of the raw molten aluminum to form small particles prior to activation. Activated aluminum comprises approximately 2.5% lithium hydride and is generated under precise conditions involving precipitation of dissolved LiH on the aluminum particle surfaces, vaporization of the solvent, and placement in a high-temperature environment (utilizing an oven) and an argon atmosphere for a few hours preventing any reaction between the aluminum and oxygen. Following the activation of aluminum, it can be stored and it is ready for use.

The report will focus on both the life cycle cost and the energy aspects of aluminum production. The costs and energy considerations mainly revolve around aluminum. To confirm that the chemical reaction has high efficiency and is cost effective, it is crucial to comprehend both the energy and production efficiency related to energy life cycle. This project will specifically address these concerns, placing a focus on energy requirements within the context of aluminum production and powder atomization of aluminum.

Aluminum Production

Aluminum is made of minerals containing the aluminum ion. Bauxite, the primary raw material for aluminum may contain several minerals, the most common of them are Gibbsite $Al(OH)_3$, Boehmite $Al_2O_3 \cdot H_2O$, and Diaspore $AlO(OH)$ [3] . Raw bauxite

undergoes Bayer process to create pure alumina (aluminum oxide) Al_2O_3, the major component for further aluminum production.

The most common method of alumina processing into aluminum is the Hall-Heroult process, which is a method that involves electrolysis or smelting of alumina with molten cryolite mineral, sodium aluminum fluoride (Na_3AlF_6). Cryolite is used as a solvent for bauxite in the electrolytic production of aluminum. This process makes the aluminum industry as one of the largest consumers of energy and therefore has a significant impact on the environment.

The energy requirement of aluminum production is relatively high. It is typically higher than other metals production due to the difficulty of extracting aluminum from its ore and the need for high temperatures in the smelting processes. In practice, it is even significantly higher than the minimum theoretical requirements as presented in Figure 1, taken from [4].

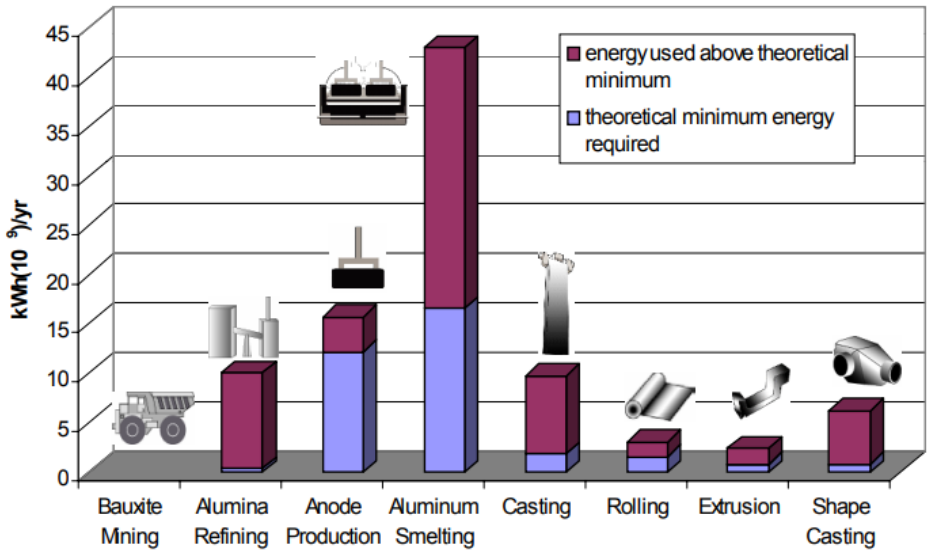

Figure 1: Annual energy used in aluminum products manufacturing [4]

Efforts to improve the energy efficiency of aluminum production have focused on reducing the amount of energy required to produce a unit of aluminum. This has been achieved by more efficient technologies, such as prebaked anodes, and the implementation of energy

management systems. The environmental impacts associated with aluminum production include greenhouse gas emissions, air pollution, and water usage. The industry has made significant efforts to reduce its environmental footprint, with initiatives such as the development of more sustainable processes, the use of renewable energy sources, and the implementation of waste reduction and recycling programs. In this report we will discuss the energy and life cycle cost of aluminum.

Primary Aluminum:

Primary aluminum is obtained through a two-step process: In the Bayer process, bauxite is refined into aluminum oxide. Next, in the Hall-Héroult process, aluminum oxide is electrolyzed to produce primary aluminum metal. After these two processes, the next step in aluminum production involves refining and processing the primary aluminum obtained from the reduction cells. This includes alloying the aluminum with other metals to achieve desired properties, casting it into various forms like ingots or components, applying heat treatments, further fabrication into products through methods like extrusion or machining, surface treatments for improved properties or appearance, and rigorous quality control measures to ensure the final aluminum products meet required specifications. The total amount of energy estimated in 2003, for primary aluminum production from bauxite was about 23.78 $\frac{kWh}{kg}$ [4].

Bayer process: The Bayer process is a hydrometallurgical method used to extract aluminum oxide (alumina) from bauxite ore. The process consists of five main steps [5]:

1. Crushing, Mixing, and Desilication: Bauxite ore is crushed and milled to reduce the particle size, then mixed with a solution of caustic soda NaOH and processed in a grinding mill to produce a slurry containing $35 - 40\%$ solids. The slurry is then heated and treated with additional caustic soda to remove impurities such as silica SiO_2 and iron oxide Fe_2O_3.
2. Digestion: The purified slurry is transferred to a digester vessel where it is heated under pressure with steam to dissolve the alumina content of the bauxite. The chemical reaction that occurs is:

$$Al_2O_3 + 2NaOH + 3H_2O \rightarrow 2NaAl(OH)_4$$

3. Clarification: The resulting sodium aluminate solution is then cooled and filtered to remove any remaining solids or impurities.
4. Precipitation: The liquid is pumped through tall tanks, where seed crystals of alumina hydrate are added to promote the growth of larger agglomerated crystals. The goal is to achieve the precipitation of crystalline aluminum trihydroxide (hydrate or gibbsite) from the supersaturated liquid.
5. Calcination: The precipitated alumina hydrate is then washed, filtered, and heated to high temperatures to remove any remaining water and produce pure alumina Al_2O_3. The chemical reaction that occurs is:

$$2Al(OH)_3 \rightarrow Al_2O_3 + 3H_2O$$

Hall-Héroult Process: The Hall-Héroult Process is a primary method for producing aluminum metal from aluminum oxide (alumina) through electrolysis in specialized cells - smelting process. The process consists of five main steps [6]

1. Preparation of the Cell: Carbon anodes are dipped into a high-temperature liquid bath solution containing alumina Al_2O_3. The bath solution is typically composed of a mixture of cryolite Na_3AlF_6 and aluminum fluoride AlF_3, which lowers the melting point of alumina to about 950°C and improves its conductivity.
2. Electrolysis: A high-intensity electric current is applied to the cell, causing the alumina to break down into aluminum and oxygen ions:

$$Al_2O_3(dissolved) + \frac{3}{2}\ C(anode) \rightarrow\ 2Al(l) + \frac{3}{2}\ CO_2(g)$$

   This reaction occurs at the carbon anodes, where the oxygen ions react with the carbon to form carbon dioxide gas, which is released into the atmosphere.
3. The liquid aluminum accumulates at the bottom of the cell. It is typically siphoned off periodically and collected in a separate container.
4. Release of Carbon Dioxide: The oxygen ions react with the carbon anodes to form carbon dioxide gas, which is released into the atmosphere. This reaction helps because it helps removing the oxygen ions from the cell.

5. Continuous Operation: Fresh alumina is continuously added to the cell to maintain the reaction. The alumina is typically added to the cell through a hopper or feeder system.

A major technological shift occurred in the preparation of carbon anodes for aluminum production, transitioning from the Søderberg process to the "prebaked" process. In the Søderberg method, the anode is not pre-baked separately. It is formed in the pot, and the green paste gradually becomes a baked anode while moving from top to bottom within the pot. The quality of Søderberg anodes is lower than that of prebaked anodes, resulting in lower current efficiency and higher pot voltage requirements. The Søderberg process has been largely replaced by the "prebake" system, where anodes are prepared outside the cell and baked in a dedicated anode baking furnace at a different location to better control emissions and enhance environmental friendliness.

To put the energy requirements into perspective we can see the process flow diagram in **Error! Reference source not found.**. The following estimates are based on annual field data of global aluminum industry, summarized by International Aluminum Institute in [7]. The most comprehensive data were available for 2019 and are presented below. For comparison, we also present the most recent data of total energy consumption from 2022.

Approximately 5.13 $tons$ of Bauxite are necessary to yield just one ton of aluminum. This initial raw material is subjected to the Bayer process, which transforms it into Alumina. The energy consumption associated with this conversion process is substantial, estimated at about 10,500 MJ per ton of Alumina produced. About 1.9 ton of alumina is required to produce 1 ton of final aluminum. Adjusting the energy consumption of alumina production to this value we get about 19,900 MJ per 1 ton of final aluminum.

Following the transformation of Alumina, the next crucial stage in aluminum production is smelting, and this is where a significant portion of the energy is consumed. On average, across various smelting technologies, the energy consumption during this step is estimated at around 51,500 $MJ\ per\ ton$ of final aluminum produced [7]. In total, the energy consumption for the entire production process adds up to 71,400 $MJ\ or$ 19,833 kWh for every ton of aluminum manufactured. This underscores the energy-intensive nature of

aluminum production, which is a critical consideration in assessing its environmental impact, sustainability, and cost. Compared to 2003 data that were previously mentioned, $23.78\ \frac{kWh}{kg} =\ 23{,}780\ \frac{kWh}{ton}$, we see more than 15% energy savings in 20 years.

Based on the most recent summary, available online at [8], we can estimate total energy consumption by primary aluminum production process by about 16,900 kWh per 1 ton of final aluminum, resulting in additional 15% savings over just last 3 years.

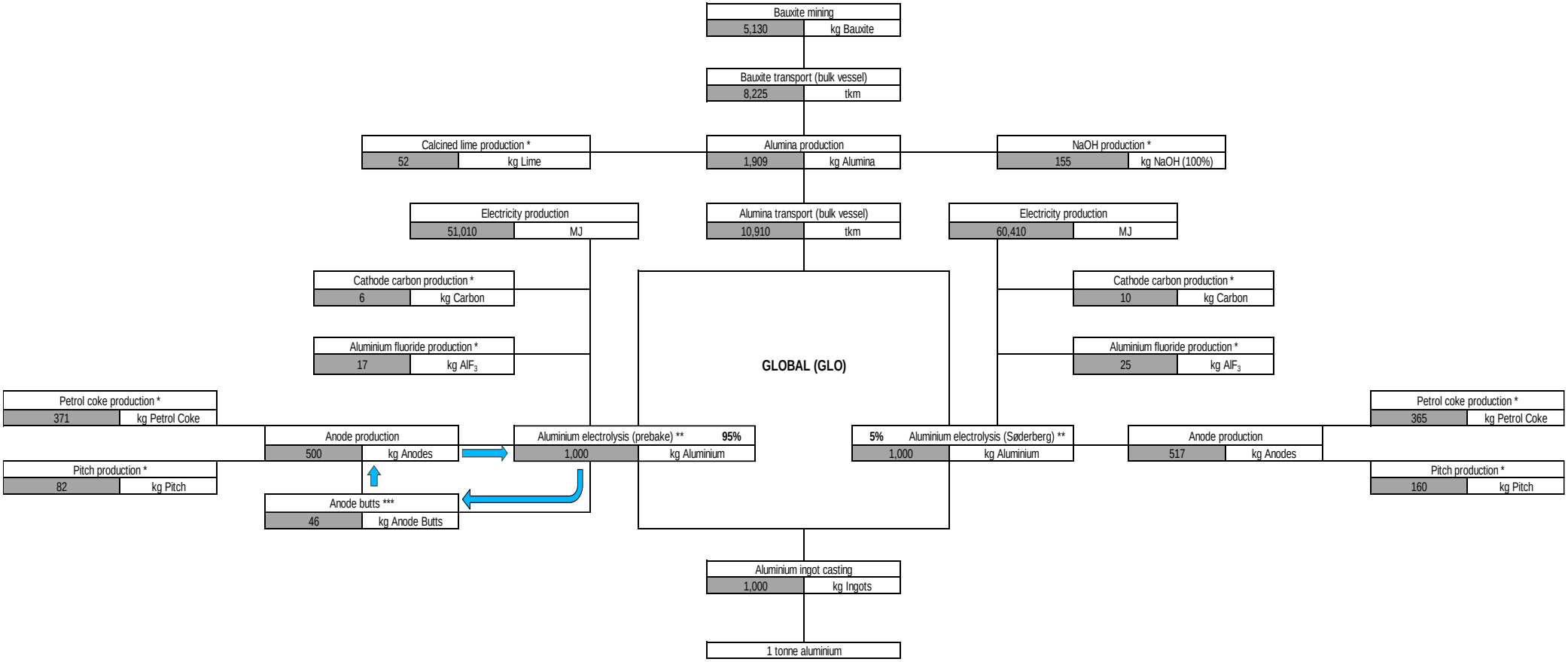

Figure 2: Life cycle of primary Aluminum production (data from IAI 2019 survey) [7]

Recycled Aluminum (secondary aluminum):

Secondary aluminum production starts from recycling used aluminum products. The aluminum scraps are separated according to their chemical composition, or their alloy, and then they are melted and cast into an ingot. According to [4], secondary aluminum consumes about 6% of the energy required to produce primary aluminum which comes to 1.427 $\frac{kWh}{kg}$ in 2003.

Around 100 $million\ metric\ tons$ of aluminum, both primary and secondary are produced annually. Aluminum offers sustainability benefits through its low mass density, reducing energy consumption in various applications such as lightweight transport and construction. It also provides efficient electrical conduction with conductivity close to pure copper but with less mass. However, aluminum production emits greenhouse gases, including carbon dioxide, methane, and nitrous oxides, contributing to approximately 3% of global emissions. Aluminum from primary production generates about 12– 16.5 ton of greenhouse gas per ton of metal produced. The high carbon footprint is attributed to the reliance on fossil fuels for electricity used in electrolysis [9]. CO_2 is primarily generated directly through the oxidation of the carbon anode during the smelting process, approximately 1.16 $tons$ of CO_2 per ton of aluminum, as indicated by the electrolysis chemical equation. This point is noteworthy, as the environmental impact associated with electricity production can be restrained by using alternative energy sources, such as hydroelectric power, potentially reducing emissions.

On the positive side, aluminum is infinitely recyclable. Around 75% of all aluminum ever produced is still in use. Recycling aluminum significantly reduces energy consumption compared to primary production from bauxite ore. Remelting aluminum scrap requires only 6% of the energy needed for primary production, resulting in lower carbon emissions. The potential for recycling to improve aluminum energy and carbon balance is substantial.

Cost of Aluminum Production

Primary Aluminum:

The cost breakdown and field data presented below is taken from [10]. The cost of alumina, representing approximately 40 percent of the total cost, is determined by the global market including shipping costs to the smelter. Anode and bath material costs are calculated as a weighted average based on their respective input groups, also reflecting global prices. Labor costs are initially measured in the local currency and then converted to US dollars using the relevant exchange rate. Furthermore, the cost of electricity is provided by CRU. CRU is a leading business intelligence firm specializing in the analysis of the global metals, mining, and fertilizer industries. It is a weighted average that factors in both an internal transfer price (self-generated electricity) and a contract price, with the weights corresponding to the input shares of total electricity consumption at the smelter level. The contract price can be either fixed or linked to the LME (London Metal Exchange) three-month price of aluminum.

The cost of smelting varies by region. For instance, the Africa and Middle East region benefits from abundant natural gas resources, resulting in cost-effective electricity for aluminum smelters. In Oceania, affordable electricity is primarily derived from coal. Additionally, specific areas in North America, particularly in Canada, enjoy economical electricity generated from hydropower. The variation in the availability of favorable long-term contracts between utility providers and smelters, alongside other factors influencing energy costs, provides additional insights into the variations in costs depicted in Figure 3, note that the data are based on 2003 prices.

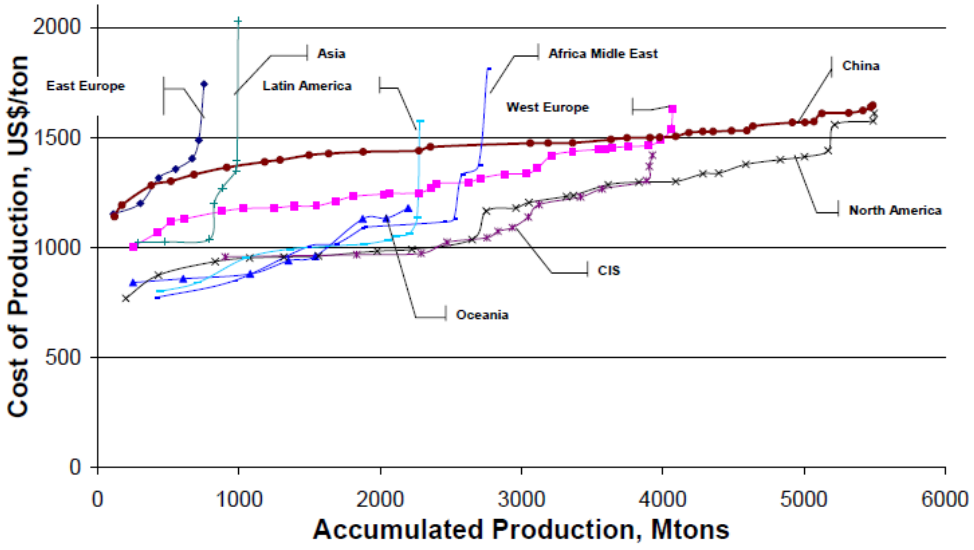

Figure 3: . Regional Variable Cost of Production per Ton of Primary Aluminium (2003 data)

Secondary Aluminum:

In many metal markets, such as copper, the secondary metal price typically follows a linear pattern closely linked to the primary metal price, with the latter often setting an upper limit for the former due to its broader range of applications. However, the aluminum market, particularly in Germany and several European countries, presents a unique scenario where, at times, the secondary aluminum price has exceeded the primary aluminum price [11]. This unusual trend can be attributed to the inherent limitations of pure primary aluminum, which requires alloying with other materials to become suitable for various applications, notably in castings. Furthermore, even in the face of rising primary aluminum prices, the demand for secondary alloys does not experience a substantial increase, mainly due to the restricted substitutability of secondary aluminum in the production of certain products. Additionally, the secondary price and scrap prices exhibit a strong correlation and considerable volatility, with instances of the German secondary producer price reaching both highs and lows in real terms. The margin between scrap and secondary prices suggests reducing industry profitability and raises concerns about the potential scarcity of aluminum scrap material. As we can see in Figure 4 the medium price of real secondary aluminum from the 90's is around 40 $\frac{ct}{lb}$ which means 880 $\frac{\$}{ton}$.

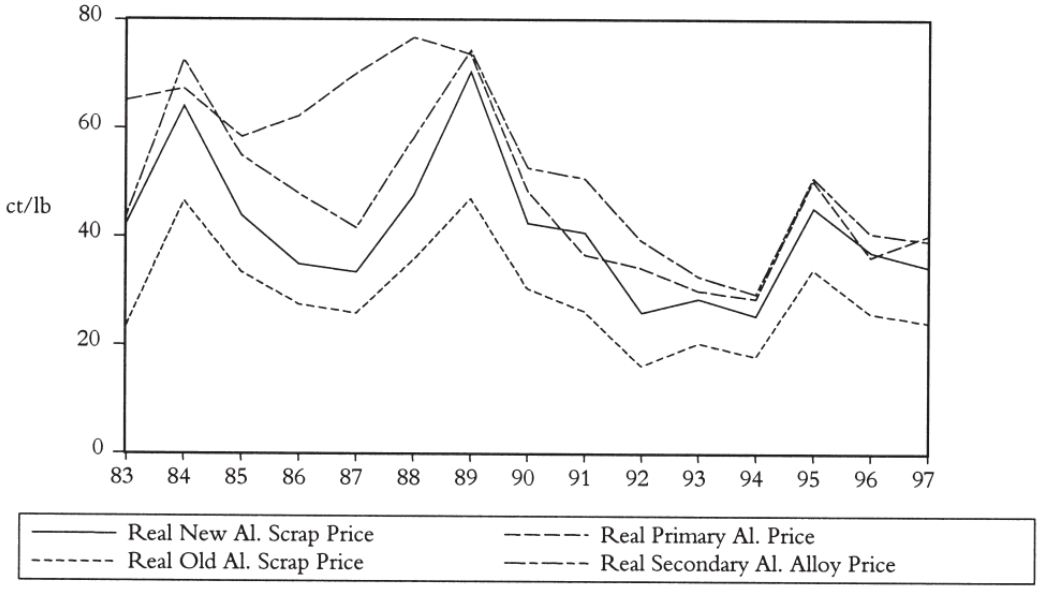

Figure 4: German aluminum metal producer prices 1983–97 (Real ct/lb The World Bank G-7 deflator is used to calculate real prices, with 1980 as the base year.)

The largest contributor to the production cost of secondary aluminum is the raw materials (old and new scrap) that accounts for up to 70 percent of total variable cost. New scrap arises during the manufacturing of aluminum products. Old scrap refers to those products collected after disposal by consumers. To reach the required quality of the remelted aluminum, some additional materials like silicon, copper and magnesium are added during the manufacturing process. These materials can contribute up to 7% of the raw material cost.

An increasingly important cost factor is the "environmental costs". These costs include different charges to reduce various kinds of environmental impact like air and water pollution, noise, salt slag and others. All these costs vary in different countries across the world, depending on laws and regulations. Hence, total environmental costs are hard to estimate, but could in some countries, reach 20 percent of total cost.

Powder Atomization

The application of aluminum for hydrogen production via the reaction with water, often requires powdered aluminum to enhance the overall reaction rate due to the much larger surfaces compared to a bulk metal.

Because of the ease with which a liquid can be broken down into droplets, atomization has become the prevalent method of Powder production of a variety of metals and their alloys (non-ferrous metals) [12]. The atomization allows the rapid production of a solid powder. The use of rapid solidification of melts to produce powders of various types is not only a very popular subject of investigation, but also finds wide industrial application nowadays. In our case, aluminum powder for hydrogen and electric energy production.

The simplest design of the atomizer is to let a stream of metal fall on a horizontal jet. Professor Hall patented his own design in the late 1920s when he made a type of adjacent sprayer for aluminum atomization. This basic design is still in use and has not improved much since then. A similar product was developed by VAMI, Figure 5. The working process is that gas is transferred through an annular opening around the nozzle at the converging angle. The gas flow creates the suction (exhaust) effect in the tip of the nozzle that draws the molten metal into the nozzle. The flow rate of the molten metal and the powder particle size are influenced by the aspirating force, the nozzle metal opening diameter, and the vertical distance between the nozzle and the molten metal level.

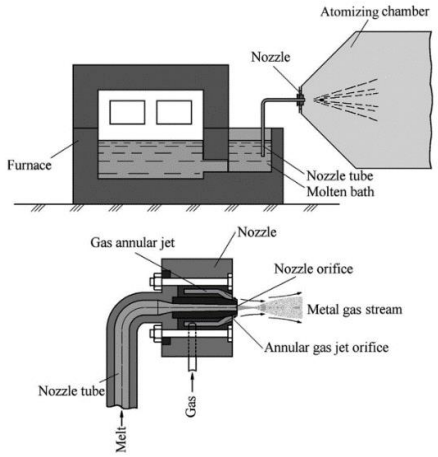

Figure 5: VAMI ejection nozzle design with horizontally molten metal stream [9]

This atomizer is designed to make contact between the liquid metal stream and the gas in order to create an efficient breakup of the liquid, resulting in finer powders. this method is most used for aluminum and other metals with a low melting point. The jet stream can be operated vertically upwards or downwards or in a horizontal position. It is important to note that careful planning of the sprayer is required to prevent the metal from freezing by the gas jet at the exit, which can lead to solidification at the tip of the nozzle.

There are many other gas atomizer designs. They can be classified as free fall, confined or closed nozzles and internal mixing. The closed nozzle design is a method that is easy to operate but is not suitable for preparing fine powders.

Confined Nozzle Designs:

This nozzle design enables an increase in the production of powder with a median particle $diamerter\ of\ 40-60\ \mu m$ by optimizing the gas velocity and density at the point of contact with the metal stream. However, the use of these units may result in the solidification of the molten metal at the nozzle's tip. Additionally, the gas stream~~'s~~ interaction with the nozzle tip can generate either a negative or positive pressure, ranging from a negative pressure that significantly magnifies the flow rate of the molten metal, to a positive pressure that is sufficient to halt it and cause gas to blow into the tundish. As a result, it is crucial to exercise caution when configuring sealed nozzles and maintaining control during the atomization process. The WIDEFLOW gas atomizer, which operates on the principle of a confined nozzle, is presented in a linear configuration in Figure 6. This atomizer composed of two chambers: a high-pressure chamber (autoclave) containing the melt, and a low-pressure atomization chamber divided by a linear Laval gas nozzle. Main characteristics of the WIDEFLOW atomizer are summarized in

Table 3. The pressure difference between these chambers drives the gas-accelerated flow through the converging linear Laval nozzle until it reaches sonic velocity, which occurs when the pressure ratio surpasses the critical value. The exceptionally high kinetic energy of the gas flow at ultrahigh velocities is efficiently transferred to atomize the thin melt film. According to Schulz's findings [13], utilizing nitrogen or argon at pressures of $2.0-2.5\ MPa$ can achieve mean particle diameters of approximately 10 μm.

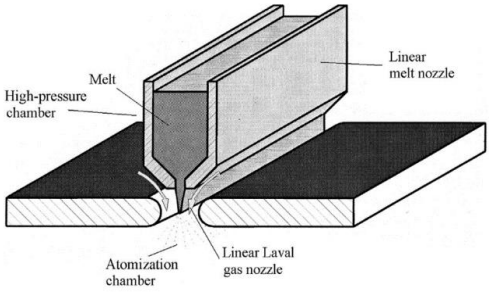

Figure 6: Simplified drawing of the WIDEFLOW confined linear nozzle design [11]

Table 3. Main Characteristic Data for WIDEFLOW gas atomizer [13]

Maximum pressure with autoclave	2.6 MPa
Maximum pressure without autoclave	1.3 MPa
Maximum atomizing gas throughput	2000 $\frac{Nm^3}{h}$
Nominal vacuum pump suction rate	400 $\frac{Nm^3}{h}$
Melting crucible	$volume$: 60 $l, approxmitly$ 300 kg
Induction heating melting crucible	$1000 - 2000$ Hz $switchable$, 270 kW
Tundish volume	$up\ to$ 8 l
Atomizing gases	$N_2, Ar, O_2, He(on\ request)$
Gas supply tanks storage capacity	$for\ N_2$: 13.700 Nm^3 ; $for\ Ar$: 8.650 Nm^3
Powder product materials	stainless, HSS, superalloys, intermetallics, copper, aluminum, magnesium alloys, precious metals

Nanoval Nozzle Design:

The Nanoval nozzle design employs friction forces between the atomization gas and the liquid to disintegrate a metal melt stream. By ensuring that the metal stream remains extremely thin and is directed straight into the nozzle throat, this design has the capability to generate exceptionally fine powders. A comparison of mean particle sizes between the

Nanoval design and the conventional confined nozzle design is depicted in Figure 7, illustrating the relationship between mass median diameter and specific gas momentum.

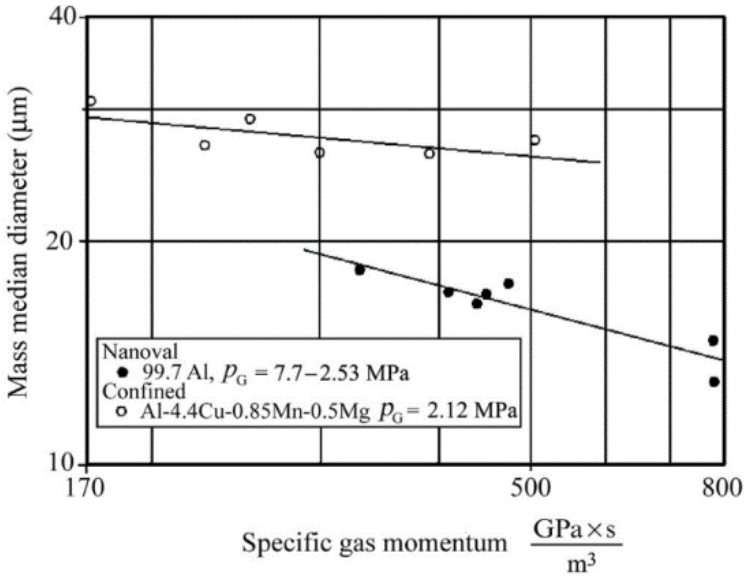

Figure 7: Comparison of mean particle sizes by Nanoval and conventional confined atomizing nozzle designs. [11]

Pressure-Swirl Hybrid Pre-Filming Atomizer:

This atomizer incorporates a combination of pressure-swirl atomization and ring-gas atomization techniques. The atomization process involves the generation of a thin film and then followed by atomization through gas jet action. The key components of the powder atomization unit include the pressure-swirl-metal chamber, atomization chamber, and gas recirculation system, as shown in Figure 8. Through the application of excess pressure, the melt flows tangentially into the swirl chamber and exits through a small cylindrical hole (D_L), forming a swirling hollow cone film of molten metal. Subsequently, the film is atomized by gas jets emitted through orifices (D_G). By heating to 373 K, a gas pressure of 1.0 $[MPa]$ (using nitrogen), a mass gas-to-metal ratio of 1.3, and maintaining a melt flow rate ranging from $160 - 190\ \frac{kg}{h}$, spherical tin powders with a median diameter of $10 - 20\ \mu m$ and a standard deviation below 2 were successfully produced.

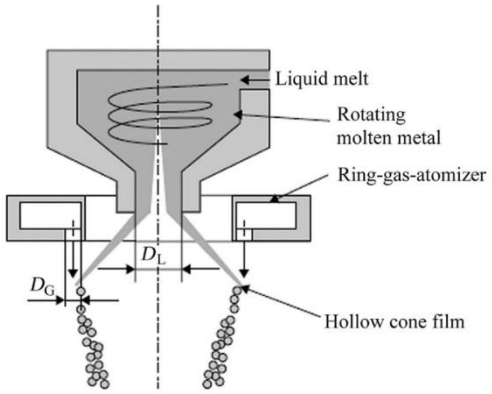

Figure 8: Pressure-swirl hybrid pre-filming atomizer [11]

Process Parameters:

In conventional gas atomization processes, the atomization pressures typically range from $0.5 - 4\ MPa$, and gas velocities within the nozzles range from Mach $1 - 3$. However, in free-fall atomizers, the gas velocities in the impingement zone generally decrease to around $50 - 150\ \frac{m}{s}$ (for air or nitrogen). The powders produced through gas atomization are typically spherical in shape, exhibiting a lognormal size distribution. The average particle sizes usually fall within the range of $10 - 300\ \mu m$, with a standard deviation of approximately 2. The oxygen content is typically around 100 ppm. The production of air-atomized powders, particularly zinc, aluminum, copper, tin, lead, and copper alloys, likely exceeds 400,000 tons per year. Air atomizers operate continuously for extended periods of time, sometimes running around the clock. Multi-nozzle systems are often utilized to enhance yield in aluminum and zinc atomization processes. In conventional inert gas or air atomization, the metal flow rates through single orifice nozzles typically range from $1 - 90\ \frac{kg}{min}$. The capacity of atomization plants varies from small laboratory-scale units to large-scale facilities. In conventional atomizers, the gas flow rate typically ranges from $1 - 50\ \frac{m^3}{min}$ at pressure levels of $0.35 - 4\ MPa$. The degree of superheating of the molten metal, which refers to the temperature difference between the melting point and the temperature at which the metal is atomized, is usually around $75 - 150\ K$. In gas atomization with inert gas, the cost of gas consumption is significant, and finding ways to promote gas reuse through circulation is essential, particularly for large-scale facilities. In practice, for a given

gas nozzle design and size, the mean particle size is controlled by the pressure of the atomizing medium and the rate at which the melt flows. For all nozzles, the gas velocity typically reaches its maximum at sonic velocity, which is approximately 300 $\frac{m}{s}$ for nitrogen and argon, at the narrowest section of the nozzle, given that the upstream gas pressure is at least 1.9 times greater than the external pressure. As a result, the mass flow rate of the gas (Q) depends on the gas pressure, temperature, and nozzle area. Under ideal conditions, assuming zero velocity at the entrance side of the nozzle, the gas flow can be expressed as:

$$Q = \omega \cdot \left(\frac{2}{k+1}\right)^{\frac{k+1}{2(k-1)}} \cdot \frac{p\sqrt{2g}}{\sqrt{RT}}$$

In the equation, ω represents the cross-sectional area of the gas nozzle at the exit, k is the ratio of specific heat at constant pressure to specific heat at constant volume $\left(\frac{C_p}{C_v}\right)$, p represents the gas pressure in the reservoir, T represents the temperature in the gas reservoir, R is the gas constant, and g represents the acceleration due to gravity.

If we were to develop the expression in metric units, we would get a little different equation. For a flow through a choked nozzle, we can use the appropriate formula in a rocket engine where P_c is the pressure in the combustion chamber, A_t is the cross section of the throat and R is the specific gas constant:

$$Q = \frac{P_c \cdot A_t}{C^*} \quad where \quad C^* = \frac{1}{\Gamma}\sqrt{RT} \quad where \quad \Gamma = \sqrt{k}\left(\frac{2}{k+1}\right)^{\frac{k+1}{2(k-1)}}$$

$$\Rightarrow Q = \frac{P_c \cdot A_t}{\sqrt{RT}} \cdot \sqrt{k}\left(\frac{2}{k+1}\right)^{\frac{k+1}{2(k-1)}}$$

To evaluate gas efficiency, a comparison based on the amount of powder surface generated per unit volume of gas consumed can be utilized. This criterion takes into account the increased gas consumption requirements associated with higher gas pressures when producing finer powders. When comparing confined nozzle designs with consumption designs, confined nozzles tend to exhibit higher efficiencies at a similar gas-to-metal ratio.

A simple equation can be employed to express δ_m the dependence of the median particle size on gas/metal ratios:

$$\delta_m = \frac{k}{\sqrt{\frac{G}{M}}}$$

Here, k represents a constant specific to the process, and $\frac{G}{M}$ represents the gas-to-metal ratio, which can be measured in terms of kilograms of gas per kilogram of metal or cubic meters of gas per unit mass of metal $\left(\frac{m^3}{kg}\right)$.

Models of Gas Atomization:

The assumption of all the models is that superheated metal melts may be considered as Newtonian fluids. It is important to note that the models and equations used in the book [12] and presented here are partially based on non-specified units.

- A model for a three-step process of droplet formation developed by Dombrowski and Johns [14] is shown in Figure 9.

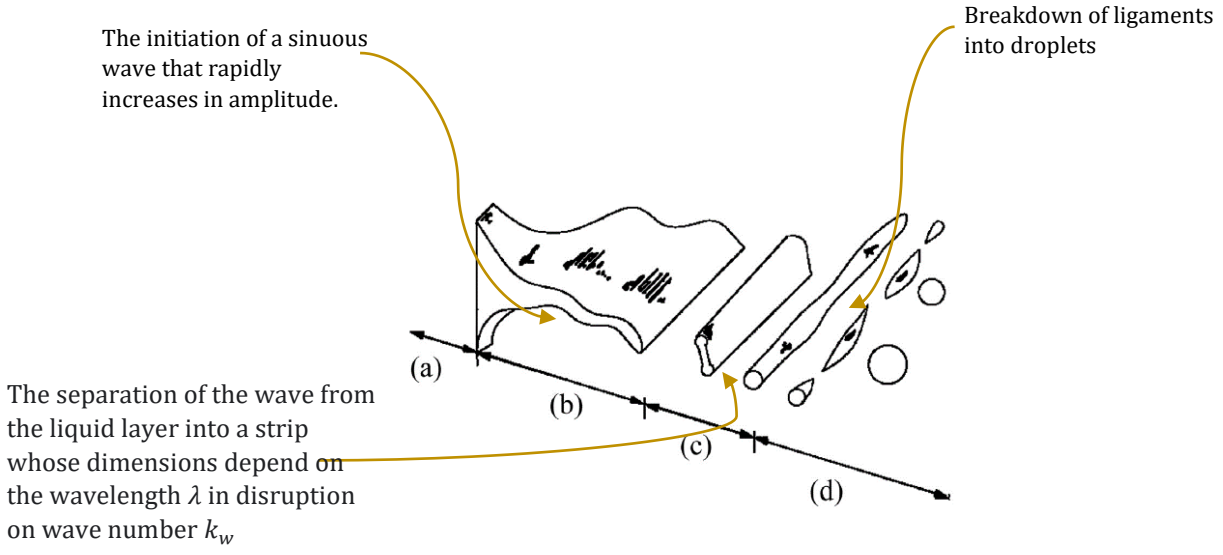

Figure 9: The droplets formation steps by [14]

- In Bradley's mathematical model (capillary wave model) [15] the liquid is in horizontal infinitely deep phase, initially unmoving and being swept by a compressible gas phase with

a uniform velocity parallel to the liquid surface. In the first stage of the breakup Rayleigh instability is used, (in a breakup of the ligament into spherical drops). In the second stage of atomization, Bradley suggested that the ligament diameter D is related to the fastest growing wavelength $\lambda_{\max}$ that is equal to $\frac{2\pi}{k_{\max}}$. From here he got the resultant droplet diameter [15]:

$$\delta = \frac{2.95\sigma_m}{L\rho_g a^2} \; when \; L = \frac{k_{max}T}{\rho_g a^2}$$

- σ_m *is the liquid surface tension* $\left[\frac{N}{m}\right]$
- ρ_g *is* the density of the gas $\left[\frac{\text{kg}}{\text{m}^3}\right]$
- νg is the sonic gas velocity $\left[\frac{\text{m}}{\text{s}}\right]$
- a *is the sonic velocity* $\left[\frac{m}{s}\right]$

- In the capillary and acceleration wave model of Ingebo [16] the major role is given to the Reynolds and Weber numbers:

$$Re_L = \frac{\rho_L(v_g - v_m)^2 d_0}{\mu_L} \; , We = \frac{\rho_g {v_g}^2 \, d_0}{\sigma_m}$$

- ρ_L *is the density of the melt* $\left[\frac{kg}{m^3}\right]$
- d_0 *is the melt stream diameter* $[m]$
- μ_L *is the dynamic viscosity* $\left[\frac{kg}{s \cdot m}\right]$
- $(v_g - v_m)$ *is the speed difference between the gas and the melt* $\left[\frac{m}{s}\right]$

The resulting Ingebo equation [16] is:

$$\frac{d_0}{\delta_m} = c_0(We \cdot Re_L)^m \rightarrow \delta_m = 37 d_0 (We \cdot Re)^{-0.4} \; ; (c_0 = 0.027 \; \& \; m = 0.4 \; for \; We \cdot Re > 10^6)$$

- The model of Ternovoy and his colleagues is based on the "modified capillary wave model in melt atomization" of Ingebo. With the assumption of atomization of a free melt stream by an annular gas jet with a hollow cone of metal formation. They managed to come up with a semiempirical formula for the droplet diameter as follows:

$$\delta_m = \frac{1.88 v_m^{0.4} \rho_m^{0.2} d_m^{1.26}}{\gamma^{0.026} \rho_g^{0.17} R_{tr}^{0.63} v_g^{0.34}} \cdot \frac{gh\rho_m + \Delta p}{gh\rho_m - 2\Delta p} \cdot \left(\frac{G_m}{G_g}\right)^{0.3}$$

- $dm\ is\ the\ melt\ jet\ diameter\ at\ the\ exit\ of\ the\ melt\ nozzle\ [m]$
- $R_{tr}\ is\ the\ film\ opening\ radius\ in\ the\ position\ of\ toroidal\ thickening\ on\ its\ periphery\ [m]$
- $g\ is\ the\ acceleration\ of\ gravity\ \left[\frac{m}{s^2}\right]$
- $h\ is\ the\ melt\ height\ in\ the\ tundish$ [m]
- $\Delta p\ is\ the\ pressure\ differential\ between\ the\ furnace\ chamber\ and\ the\ nozzle\ [Pa]$
- $G_m\ is\ the\ melt\ mass\ flow\ \left[\frac{kg}{s}\right]$
- $G_g\ is\ the\ gas\ mass\ flow\ \left[\frac{kg}{s}\right]$
- $\gamma\ is\ the\ specific\ surface\ energy\ (surface\ tension) of\ a\ melt\ \left[\frac{J}{m^2}\right]$

The model for pressure-swirl atomization that has conical film of melt created by the pressure swirl nozzle and shaped by centrifugal forces, is atomized by high-velocity gas jets. The model is based on [16] and a new extension for the last stage. This can be shown as a four-stage process in Figure 10:

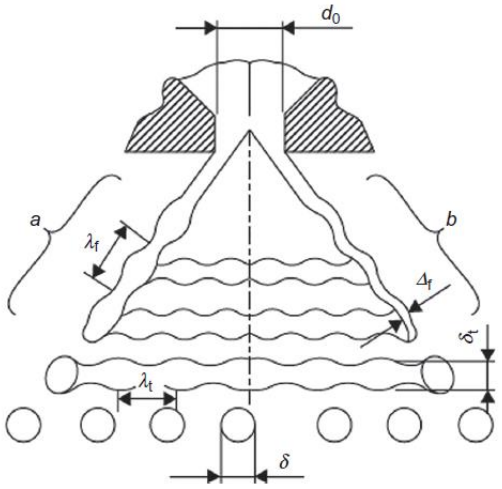

Figure 10: Stages in the formation of droplets in a swirl nozzle injector

1. Unsteady wave propagation along and across to velocity due to induced oscillation processes by external and internal factors. The instability wavelength λ_f. Depending on the physical properties of the liquid and gas, two schemes are suggested: A

thickening of a film in toroidal form in accordance with the wavelength (a) and when a film is just bending (b):

2. Formation of a liquid torus on the peripherals of a film because of transmission of a longitudinal wave with the fastest growing amplitude.
3. Transmission of the instability of the toroidal peripheral area.
4. The final stage differs from the other stages because it consists of secondary atomization of previously broken-up ligaments (torus or drops in dependence on atomization conditions) under the action of a high gas pressure jet.

Based on this model, a formula for the definition of particle diameter was suggested:

$$\delta = k\varphi^{0.46} \cdot \frac{\nu_m^{0.17} \rho_m^{0.08} \sigma_m^{0.38} d^{0.92}}{R_f^{0.46} \rho_g^{0.46} \nu_g^{0.92}}$$

- $k\ is\ the\ coefficient\ of\ the\ nozzle\ geometry$
- $\varphi\ is\ the\ unfilled\ coefficient\ for\ the\ melt\ nozzle\ orifice\ of\ d\ diameter$
- $\nu_m\ is\ the\ kinematic\ viscosity\ of\ the\ melt\ \left[\frac{m^2}{s}\right]$
- $\nu_g\ is\ the\ kinematic\ viscosity\ of\ the\ gas\ \left[\frac{m^2}{s}\right]$
- $d\ is\ the\ radius\ of\ the\ nozzele\ [m]$
- σ_m is the surface tension of the melt $\left[\frac{N}{m}\right]$
- $R_f\ is\ the\ radius\ of\ the\ film\ at\ the\ point\ of\ break\ up\ [m]$

Summary

The project presents a comprehensive overview of key processes and factors of aluminum production, with a specific emphasis on the energy and life cycle cost. For primary aluminum, the energy requirements in 2003 stood at 23,780 $\frac{kWh}{ton}$, decreasing to 16,900 $\frac{kWh}{ton}$ in 2022. With an accumulated production of 4,000 $Mtons$ in Western Europe in 2003, the production cost for primary aluminum was 1500 $\frac{\$}{ton}$. In contrast, secondary aluminum consumes approximately 6% of the energy needed for primary aluminum, amounting to 1427 $\frac{kWh}{ton}$ in 2003, and the average market price for real secondary aluminum in the 90's was around 880 $\frac{\$}{ton}$.

The project also explores the differentiation between primary and secondary (recycled) aluminum, clarifying the production processes linked with primary aluminum, such as the Bayer process for refining bauxite into aluminum oxide and the Hall-Héroult process involving specialized cell electrolysis. Additionally, the project delves into mathematical and experimental models for gas atomization, focusing on non-ferrous metals, particularly aluminum.

Special attention is given to different atomization techniques of molten aluminum for the production of aluminum powders.

Motivated by advancing research on the reaction between aluminum and water for hydrogen production, this project serves as a base of knowledge, aiming to ongoing research into the process, with the goal of validating its efficiency and utility.

References

1. Rosenband, V. and Gany, A., "Application of Activated Aluminum Powders for Generation of Hydrogen from Water", *International Journal of Hydrogen Energy*, Vol. 35, Issue 20, Oct. 2010, pp. 10898-10904, ISSN 0360-3199.

2. Elitzur, S., Rosenband, V., and Gany, A., "Study of Hydrogen Production and Storage Based on Aluminum-Water Reaction", *International Journal of Hydrogen Energy*, Vol. 39, 2014, pp. 6328-6334.

3. Williams, F. and Raahauge, B., "Smelter Grade Alumina from Bauxite, History, Best Practices, and Future Challenges ", *Springer Series in Materials Science*, Vol. 320, Gewerbestrasse, Switzerland, 2022, chapter 1, pp. 1-15.

4. "U.S. Energy Requirements for Aluminum Production, Historical Perspective, Theoretical Limits and Current Practices", U.S. Department of Energy, Feb. 2007, pp. 1-30.

5. Peterson, R. and, Tabereaux, A., "Aluminum Production", Treatise on Process Metallurgy, Elsevier Ltd, Vol. 3, USA, 2014, pp. 839-917.

6. Moreira, L., Besançon, G., Ferrante, F., Fiacchini, M., and Roustan, H., "Convection-diffusion Model for Alumina Concentration in Hall-H´eroult Process", IFAC-PapersOnLine, Vol. 55, Issue 21 ,2022, pp. 150-155

7. International Aluminium Institute. Exel document recieved in private communication from International Aluminium Institute, 2019.

8. [Online] international-aluminium . https://international-aluminium.org/.

9. Raabe, D., Ponge, D., Uggowitzer, P., Roscher, M., Paolantonio, M., Liu, C., Antrekowitsch, H., Kozeschnik, E., Seidmann, D., Gault, B., Geuser, F., Deschamps, A., Hutchinson, C., Liu, C., Li, Z., Prangnell, P., Robson, J., Shanthraj, P., Vakili, S., Sinclair, C., Pogatscher, S., "Making sustainable aluminum by recycling scrap: The science of "dirty" alloys.", *Progress in Materials Science*, Vol. 128, 100947, July, 2022.

10. Blomberg, J., and Jonsson, B., "Calculating and Decomposing the Sources of Inefficiency within the Global Primary Aluminium Smelting Industry: A Data Envelopment Approach", Doctoral Thesis, ISSN 1402-1544, Luleå, Sweden, 2007.

11. Blomberg, J., Stefan, J., "Short-run demand and supply elasticities in the West European", Doctoral Thesis, ISSN 1402-1544, Luleå, Sweden, 2000.

12. Neikov, O., "Atomization and Granulation", Handbook of Non-Ferrous Metal Powders, Elsevier Ltd, 1st ed., Elsevier, 2019, pp. 102-142.

13. Schulz, G., "Ultrafine Metal Powders for High Temperature Applications Made by Gas Atomization", *Conference: 15. international Plansee seminar,* Vol. 3, Reutte, Austria, July, 2001, pp. 74-84.

14. Dombrowski, N and Johns, W. R., "The aerodynamic instability and disintegration of viscous liquid sheets". 3, *Chemical Engineering Science*, Vol. 18, Issue 3, March, 1963, pp. 203-214.

15. Bradley, D., "On the atomization of liquids by high-velocity", *Journal of Physics D: Applied Physics*, Vol. 6, 1973.

16. Ingebo, R. N., "Capillary and Acceleration Wave Breakup of Liquid Jets in Axial Flow Airstreams", NASA TP.1791, Jan, 1981.